Sol-gel derived materials as substrates for neuronal differentiation: effects of surface features and protein conformation†

Sabrina S. Jedlicka,[a] **Janice L. McKenzie,**[b] **Silas J. Leavesley,**[b] **Kenneth M. Little,**[e] **Thomas J. Webster,‡**[bc] **J. Paul Robinson,**[bdf] **David E. Nivens**[e] **and Jenna L. Rickus***[abd]

This work demonstrates the ability of sol-gel derived materials to support the differentiation of neuronal cells, and investigates the physiochemical interactions between the surface and extracellular matrix proteins as a mediator of the effects of surface features on differentiation. We have applied fluorescence resonance energy transfer (FRET) spectroscopy to study the conformational changes of human serum fibronectin, a critical extracellular cell adhesion protein, after adsorption onto native and poly-L-lysine doped sol-gel derived silica thin films and bulk materials. The global conformation of fibronectin varied dramatically between native and organically modified materials and most interestingly between thin films and bulk materials of the same chemistry. A comparison of the surface topography of thin films and bulk materials by atomic force microscopy reveals that films of native silica have surface features less than the AFM tip size (<25 nm) while bulk materials of the same precursor chemistry have features ranging from 50–100 nm in size. Fibronectin assumed an inactive, globular, solution-like state on the larger feature size bulk gels and an active, fully extended fibrillar-like state on the smaller feature size films. Neither native nor PLL-doped bulk materials could support cell growth or neuronal differentiation of PC12 cells, in stark contrast to the thin films, which supported a robust neuronal phenotype. Morphological analysis and expression levels of the neuronal proteins β-tubulin and neurofilament, in addition to the FRET data, indicate that the effects of surface chemistry on fibronectin conformation, cellular adhesion, and differentiation are dependent upon the surface topography.

Introduction

The integration of differentiated neurons into engineered devices has broad applications including implantable biomedical devices and cell-based biosensors, and requires that cells directly interface inorganic or hybrid materials. Sol-gel derived materials have recently demonstrated potential as substrates for adherent mammalian cells.[1] Here we demonstrate the ability of these materials to function as a biointerface for the differentiation of neuronal cells.

The sol-gel method of producing porous inorganic glass under biologically benign conditions[2,3] has many advantages

for producing a solid phase biointerface to cells.[1,4] The pores can be doped with a wide variety of biological molecules, self-assembled structures, and living cells to impart the material with biological functionality. Soluble proteins,[2,3] liposomes,[5–7] membrane proteins,[8] bacteria,[9,10] and mammalian cells[11,12] all remain functional after immobilization and can even exhibit increased stability compared to their free solution form. The silica matrix allows for surface modification as well as interior pore activation through liquid precursor design, post-processing, or the doping of organic polymers,[13–15] surfactants,[16] or small molecules[17] into the porous network. For a comprehensive review of biological applications of sol-gel materials see the recent article by Avnir, Coradin, Lev, and Livage.[18]

Despite the high potential for sol-gel derived glass as a culture surface and biointerface, little is known about the mechanism of effects of material properties on mammalian cells outside of the application of bone regeneration using bioactive glasses.[19] Zolkov, Avnir, and Armon recently demonstrated the effect of hydrophobicity and charge on the growth of Buffalo green monkey cells on native and organically modified sol-gel silica thin films.[1] The ability of the hybrid films to enable culture under reduced serum levels highlighted the importance of the material chemistry on the adsorbed protein layer that mediates cell–material interactions.

Preliminary work indicated that material morphology (cast bulk monoliths versus dip-coated thin films) dramatically impacts cell function in a cell-type dependent manner.[20]

[a] Department of Agricultural & Biological Engineering, Purdue University, 225 S. University Street, West Lafayette, IN 47907-2093
[b] Weldon School of Biomedical Engineering, Purdue University, 206 S. Intramural Drive, West Lafayette, IN 47907
[c] School of Materials Engineering, Purdue University, 501 Northwestern Avenue, West Lafayette, IN 47907
[d] Bindley Bioscience Center, 1203 W. State Street, Purdue University, West Lafayette, IN 47907-2057
[e] Department of Food Science, 745 Agriculture Mall Drive, West Lafayette, IN 47907-2009
[f] Department of Basic Medical Sciences, Purdue University, 625 Harrison St., 625 Harrison St., IN 47907-2026

We hypothesized that these effects are mediated by altered protein–matrix interactions at the material biointerface due to differences in surface topography between thin films and bulk monoliths. Bulk materials are typically cast from liquid precursors. The dip-coating of thin films results in additional processes including rapid evaporation and gravitational draining that induce changes in the material structure such as pore collapse within the matrix.[21] These structural differences likely translate into differences in surface features.

Optical methods including fluorescence anisotropy measurements of fluorescent probes[22] have explored the rotational dynamics and conformation of sol-gel entrapped proteins.[23,24] These findings have numerous implications including altered kinetics and stability of immobilized enzymes. More recently, similar methods have been used to elucidate interactions between peptides and silica particles as a simpler model system.[25] Few if any studies, however, have explored on sol-gel surfaces, the large global conformational changes of non-entrapped proteins, such as fibronectin, that are able to form extended and fibrillar structures.

Numerous studies of cell growth on other material types including self-assembled monolayers (SAM's),[26] polymers,[27–30] and hydrogels[31,32] have demonstrated the effects of physio-chemical properties such as chemical functional groups,[33–36] crystallinity,[30] and roughness[37] on cell adhesion and phenotypic expression. One of the first steps to occur in the process of cell adhesion is the adsorption and cellular manipulation of extracellular matrix (ECM) proteins, such as vitronectin, laminin, and fibronectin. The adsorption and resultant conformation of these proteins is influenced by the surface properties of the material,[34,35,38,39] modulating the development, organization, maintenance and repair of tissues.[40] Surface chemistry,[34,38,41–43] hydrophobicity,[43] and topography[30,37,44] all affect the amount of protein adsorbed as well as the cellular response in a wide variety of cells.[33,35,36,45,46] Protein conformational changes expose critical binding sites which may provide signals to the attaching cells; dictating future cellular events, including migration, differentiation, or proliferation.[47]

In this study, we demonstrate that under conditions of identical synthesis chemistry, processing-dependent changes in surface features of sol-gel silica materials have dramatic effects on the biointerface, specifically the conformation of extracellular matrix proteins at the surface. These differences in material properties ultimately correlate to changes in neuronal survival and differentiation. Bulk and thin film materials of native and organically modified silica were produced and examined. We used a FRET (fluorescence resonance energy transfer)[48] technique to characterize the protein conformation at the surface of the four material types. This method recently developed by Vogel *et al.* takes advantage of the known protein unfolding pattern of fibronectin. The careful placement of fluorescent donor and acceptor probes on the protein enables measurement of the global conformation of the protein at a surface. To understand the differences in protein unfolding between the bulk materials and the thin films, atomic force microscopy (AFM) was used to examine the surfaces for comparison. Finally, to assess the cellular response

in correlation to protein conformation, we examined the ability of a neuronal cell model, PC12 rat pheochromocytoma cells, to adhere and differentiate into a sympathetic neuronal phenotype on the various sol-gel materials.

Results and discussion

Calibration of FRET

The intramolecular energy transfer of labeled fibronectin was correlated to known structural changes of fibronectin under denaturing conditions. The effect of denaturation with guanidine hydrochloride on FRET efficiency is shown in the electronic supplementary information (ESI†). The spectral characteristics generated by our methods on PEGylated slides coincide with the results obtained by previous studies.[43,48,49] The ellipticity of labeled and unlabeled fibronectin in solution at varying stages of denaturation also correlated to a previous study[43] with fibronectin beta-sheet structure remaining intact from 0–1.5 M and suddenly decreasing sharply from 1.5–4 M guanidine hydrochloride (data not shown). The sensitivity of FRET from 0–1.5 M guanidine hydrochloride is due to the expansion of fibronectin from the disruption of the intra-molecular electrostatic interactions that stabilize the molecule's overall quaternary structure.[43] Above 2 M guanidine hydrochloride, a further decrease in FRET efficiency is observed. At these higher denaturant levels, fibronectin begins to lose secondary structure and denatures rapidly.[50]

Fibronectin conformation on thin film versus bulk materials

Fibronectin conformational changes were assessed on four different surfaces and compared to fibronectin unfolding in solution. The material surfaces included tetramethoxysilane (TMOS) based bulk materials and thin films, as well as TMOS bulk materials and thin films doped with 0.01% poly-L-lysine (PLL, final concentration). PLL is a commonly used surface coating for two dimensional culture of neurons including PC12 cells[51] and has been used extensively in the patterning of neuron permissible surfaces.[52,53] PLL is generally accepted as a nonspecific adhesive polymer and is therefore not expected to have direct biological effects to the neurons beyond any influence on the physical and chemical properties of the material.

The FRET efficiency on sol-gel substrates varied dramatically with sol-gel material type (Fig. 1 A and B). The native TMOS bulk materials demonstrated a native protein structure, with 90–100% FRET efficiency. The native TMOS thin films, however, indicated a completely unfolded fibronectin state, similar to exposure to 3–4 M guanidine hydrochloride. This unfolded state indicates that the fibronectin is beginning to assume the fibrillar state necessary for integrin recognition. In previous work –OH chemical functionality (very hydrophilic) adsorbed less fibronectin, but the fibronectin molecules exhibited more integrin activity, hence the fibronectin is more unfolded.[34] On the TMOS thin films and bulk materials, the only functionality available to the fibronectin is an –OH moiety, and we might expect these materials to demonstrate a more unfolded fibronectin state. This expected finding is observed for the thin films but not for the bulk materials. The
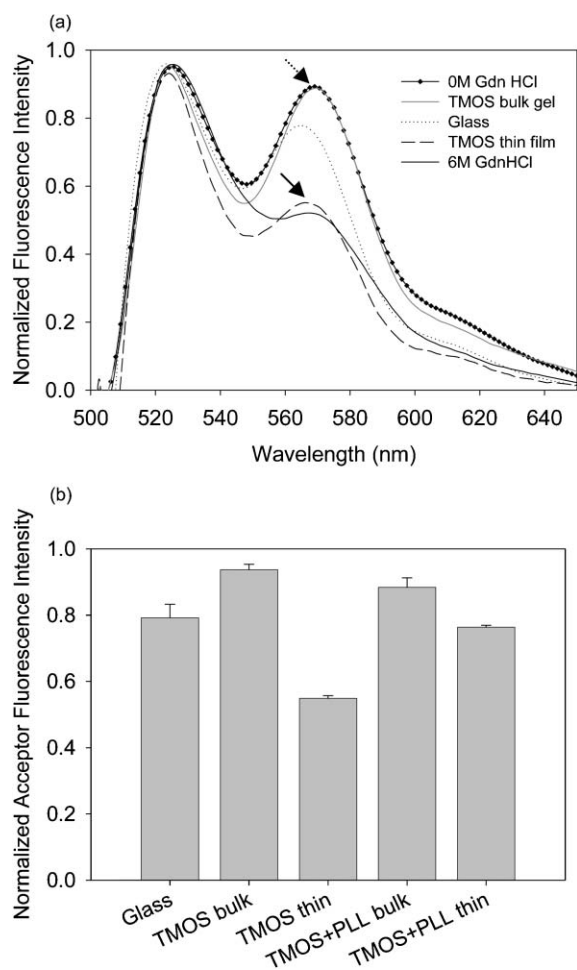
Fig. 1 Fluorescence resonance energy transfer spectra scans (a) and normalized acceptor fluorescence (b) of fibronectin adsorbed to model sol-gel surfaces. All data are normalized to peak donor emission. Bulk TMOS gels demonstrate a native globular protein conformation, indicated by the bold arrow. Thin film TMOS gels demonstrate a 55% FRET efficiency, the conformation can be correlated to complete loss of secondary structure, as determined by guanidine denaturation (dashed arrow). 0M and 6M guanidine hydrochloride solution scans are included for reference. Data on bar chart are averages $\pm$ SE of nine sol gel samples. The FRET efficiency between the bulk TMOS materials and thin films was found to be significant (student's t-test, $\alpha = 0.05$).

differences between the bulk material and thin films in FRET response can therefore not be explained by chemical functionality only and indicate that the morphology of the material has a strong impact on the effects of presented functional groups. Both surface topography[54,55] and charge density[41,56] have been demonstrated as potential additional factors affecting the fibronectin structure.

The fibronectin conformation on both sets of PLL doped materials fell in between the extremes of the globular form on the native bulk materials and the extended form on the native thin films. The PLL provides a positive charge to somewhat neutralize the negatively charged silica. Additionally, extremely hydrophobic and moderately hydrophobic surface groups (–CH$_3$ and –NH$_3$) have been shown to adsorb higher

levels of protein, but not exhibit much integrin activity until the protein concentration was high enough that the protein molecules were interacting with one another instead of the surface.[34]

The effect of PLL doping depended upon the morphology (bulk versus thin film). PLL doping had little effect on the fibronectin conformation on the bulk materials. The bulk gels both generated a high FRET ratio, and the statistical significance between the two gel types is negligible (student's t-test, $\alpha = 0.05$). In contrast, the PLL doped thin films demonstrated an increased FRET activity (more globular) in comparison to the native TMOS thin films, perhaps due to either a decreased charge density or a greater potential for NH$_3$ functionalities at the surface of the films due to the pore collapse and the exposure of the PLL.

While there is much debate over the effects of charge on protein unfolding, fibronectin may be subject to charge-induced unfolding.[41,55,56] The thin films, due to pore collapse potentially have a higher charge density than the bulk materials. The native TMOS materials, in general, have a high negative charge at physiological pH. These charges will interact with the fibronectin, possibly disrupting the ionic interactions that maintain the globular solution state.[56] As the number of electrostatic interactions increases, the possibility for electrostatic disruption is more likely, leading to protein unfolding. Monolayer coverage is critical for these forces to overcome the protein structure, and was maintained throughout the protein experiments. The PLL imparts some positive charge on the TMOS surface, and although it should not completely overcome the negatively charged TMOS surfaces, the surface is somewhat neutralized. Due to the potentially increased amount of adsorbed fibronectin due to the NH$_3$ moiety, the electrostatic disruption of fibronectin should be reduced leading to a more compact, and therefore less biologically active fibronectin conformation, as evidenced by the FRET studies.

AFM characterization of surface features of thin film and bulk materials

Due to the dramatic differences in protein conformation between the bulk materials and thin films of identical chemistries, AFM was used to determine the differences in nanostructure and topography of the sol-gel surfaces (Fig. 2). The bulk gels demonstrated a marked degree of roughness, and had large void spaces where a pore entry is apparent, regardless of sol-gel chemistry. The features on the bulk gels were approximately 50 nm in height or greater. To our knowledge, this is the first published AFM image of bulk silica gels under fluid, however, the approximate width of the features and void spaces were consistent with expected physical properties of silica sol-gel materials. The nanotopography from AFM imaging of the thin films agreed with the few published studies on sol-gel produced silica based thin films.[57,58] The thin-films demonstrated features that are on the order of the radius of tip curvature. Nanostructure features measured in height up to 25 nm and were few in number. The thin films were less rough and more consistent. The thin films were prepared from identical liquid silicate precursors, but

This journal is © The Royal Society of Chemistry 2006

J. Mater. Chem., 2006, **16**, 3221–3230 | 3223
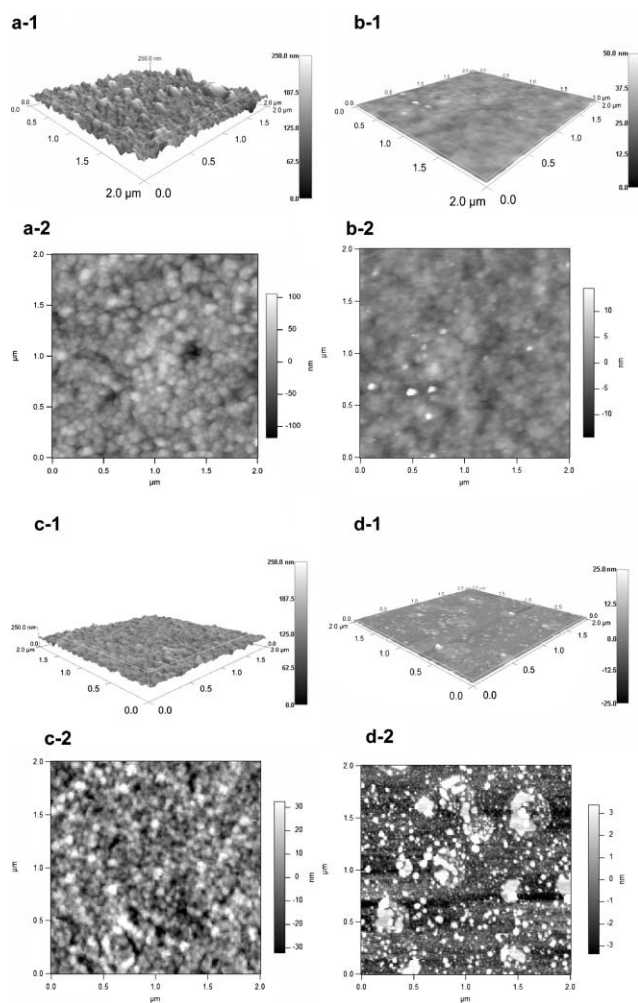
Fig. 2 Atomic force microscopy images of bulk and thin film sol-gel materials. All images were collected under tapping mode using 60 μm long bio-levers (Asylum Research). (a) Bulk native TMOS sol-gel material images (1) 2 μm, (2) corresponding height trace. (b) Thin film TMOS sol-gel material images (1) 2 μm, (2) corresponding height trace. (c) Bulk TMOS + PLL sol-gel material images (1) 2 μm, (2)cCorresponding height trace. (d) Thin film TMOS + PLL sol-gel material images (1) 2 μm, (2) corresponding height trace.

upon removal of the glass substrate from the hydrolyzed sol during processing, the gel rapidly condenses, and the pores collapse; eliminating the large void spaces, leading to a more subtle topography.[21] In addition differing degrees of syneresis could result in a higher density of hydroxyl groups on the thin films, highlighting the importance of possible interactions between processing conditions, chemical functionality and morphology.

Study of biosilification has elucidated important interactions between natural and synthetic polyamines with silica and silicate precursors.[59,60] For this reason, the impact of PLL on material morphology was also explored using AFM. As seen in Fig. 2, the PLL had little effect on the nanostructure of the sol-gel materials. Differences between the bulk and thin film surface morphology remained in the presence of PLL doping. Additionally, phase images were collected for both native TMOS and PLL doped TMOS materials. The phase contrast

between the native and modified gels was not statistically significant at the concentration of PLL used.

Fibronectin adsorbs onto most surfaces as isolated molecules or as a monolayer.[56] The fibronectin used in this study is a large 440 kDa dimeric glycoprotein that forms the atypical "hair-pin"-like structure in solution. Each 70 nm long dimer arm consists of a series of three types of globular modules, commonly referred to as "beads on a string", with each bead having an approximate Stoke's radius of 10–15 nm. The overall shape of fibronectin in physiological solution is approximately that of an oblate ellipsoid with a 10 : 1 to 15 : 1 axial ratio [43] and an approximate radius of 20–30 Å.[61] The bulk gel features are larger than the largest dimension of the globular fibronectin molecule. The size difference and feature frequency of the thin films and bulk gels may affect the interactions of the protein with the surfaces. The large size of bulk gel features and the regularity with which they occur could potentially inhibit the unfolding of fibronectin due to steric interactions and the protein may find it thermodynamically more favorable to simply "settle" into the valleys between the features. The thin films, however, with the reduced size and frequency of features may increase the rate of fibronectin unfolding due to charge induced interactions between the thin film and the molecules.

Neuronal differentiation on thin film and bulk materials

To investigate the cellular response in correlation to the protein conformation on the varying surfaces, PC12 cells were seeded onto the bulk and thin film sol-gel materials. To investigate the effect of charge and chemistry on PC12 cell response, both native and PLL doped bulk gels and thin films were used. Tissue culture plates, cleaned glass and cleaned glass with PLL coating were used as control substrates for comparison. Cells were seeded onto substrates in an undifferentiated state and induced to differentiate using 50 ng ml^{-1} nerve growth factor (NGF). NGF acts through the TrkA receptor to promote survival of the cells, *via* the mitogen-activated protein kinase pathway, ultimately leading to neurite extension.[62]

Morphological analysis of the PC12 cells grown on the various surfaces indicate a drastic impact on the differentiation and adhesion of the cells as shown in Figs 3 and 4. The cells occasionally attached and generally did not respond well to the native bulk gels. The cells died in response to the doped PLL bulk gels. Cell adhesion is primarily mediated by integrin interactions,[63] which are extremely important due to their adhesive function as well as their capacity to modulate signal transduction pathways affecting gene expression.[64] Integrins bind to several amino acid sequences located in ECM proteins, including the arginine–glycine–aspartic acid sequence (RGD) found in fibronectin and several other ECM proteins; these domains must be accessible for successful cell adhesion and subsequent processes.[40] The protein conformation on bulk materials determined using the FRET studies would indicate that the fibronectin is not in a biologically active form, and therefore, the failure of cells to adhere and differentiate on this material is consistent with the FRET data. In addition, organic modification of the bulk materials with PLL had
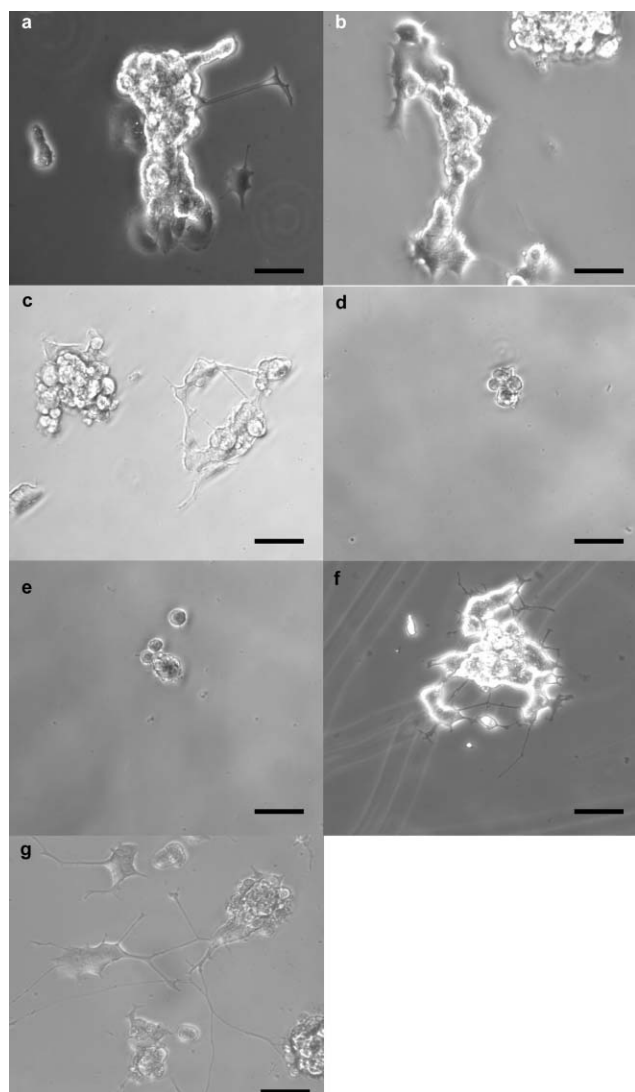
Fig. 3 Compatibility of NGF induced PC12 cells with sol-gel materials. Phase contrast images of PC12 cells exposed to 50 ng ml^{-1} NGF cultured on: (a) control tissue culture plastic plates; (b) control cleaned glass; (c) control cleaned glass coated with 0.01% poly-L-lysine; (d) TMOS bulk gel; (e) TMOS bulk gel doped with poly-L-lysine; (f) TMOS thin film; (g) TMOS thin film doped with poly-L-lysine. Scale bars represent 100 μm.

no positive effect on the growth of the cells, again consistent with the observation that PLL had no effect on the global conformation of fibronectin at the surface. Fibronectin remained in a globular biologically inactive state after PLL doping. Together these results suggest that the effects of sol-gel surface topography on neuronal cell function are mediated by protein–matrix interactions at the surface.

The cells seeded onto thin films fared significantly better. The native TMOS thin films demonstrated clusters of cells that appear to differentiate into a neuronal phenotype. The PLL doped TMOS thin films demonstrated cells that spread more evenly over the surface and in general exhibited higher numbers of differentiated cells (Fig. 5). The neurite extension also appeared to be longer (although not measured). In addition, when examining the cells under confocal fluorescence

microscopy (Fig. 4), the cell clumps consist of fewer cells on the PLL doped gels, indicating a charge effect on the cell seeding and attachment. The neurite processes and cell bodies are stained a bright green, while the nuclei of individual cells are stained a bright blue. The transmittance images are included alongside the fluorescence images, highlighting the necessity to conduct cell counting chemically rather than through visualization, as cells that appear to be individual can actually be groups of cells undergoing neuritogenesis.

The cells were examined for protein expression using an ELISA technique to stain for two neuronal markers, β-tubulin and neurofilament protein. Neurofilament proteins are the intermediate filament proteins that assemble into neurofilaments, the primary cytoskeletal element in nerve axons and dendrites. β-tubulin III exhibits neuron-specificity and may play a role in axonal growth.[65] The results for thin films are summarized in Fig. 5, along with the manual differentiated cell counts. The bulk gels are not presented as these materials did not support any differentiated cells and the neuronal markers were not present upon ELISA staining. Differentiated cell counts based on neurite extension generally correlated with neuronal marker expression levels on the different materials with the exception of the PLL doped thin films. Interestingly, cells on the TMOS films doped with PLL, expressed lower levels of protein, although more of the cells appeared differentiated, the neurite processes appeared longer, and the cells seemed to spread out more readily on the surfaces. This result was consistent for both neurofilament and β-tubulin expression.

The reduced neurofilament and β-tubulin expression in the PLL doped films could be due to either a different time course of differentiation, a different mechanism of differentiation or both. The protein expression was measured at a single time point, 14 days after introduction of NGF. Neurite outgrowth occurs at a faster rate on the PLL doped films compared to the native films (Fig. 5B and data not shown); at day 14, the two cell sets might simply be at different stages in the same differentiation process. Alternatively, the neurite outgrowth observed on both material types might be due to different differentiation processes resulting from different signaling cascades or metabolic states that are initiated or influenced by the different material properties and fibronectin conformations.

The antibodies used recognize specific epitopes on the proteins; specifically, the neurofilament antibody recognizes non-phosphorylated neurofilament triplet protein and the β-tubulin antibody recognizes the β-LC and β-SC proteolytic fragments of β-tubulin. Neurofilaments and tubulin both undergo vast post-translational modifications in response to varying differentiation states, perturbations, or degeneration. Neurofilament triplet proteins, in particular, are subject to variable phosphorylation states during stabilization of the neurofilaments.[66,67] Additionally, the β-LC fragment is the site of MAP1B binding and stabilization on the β-tubulin protein; which can reduce the affinity of the antibody to the protein.[68] Thus, the decreased protein expression may be a product of different isoforms in response to a varied differentiation stage or signaling cascade. The expression data collected in this
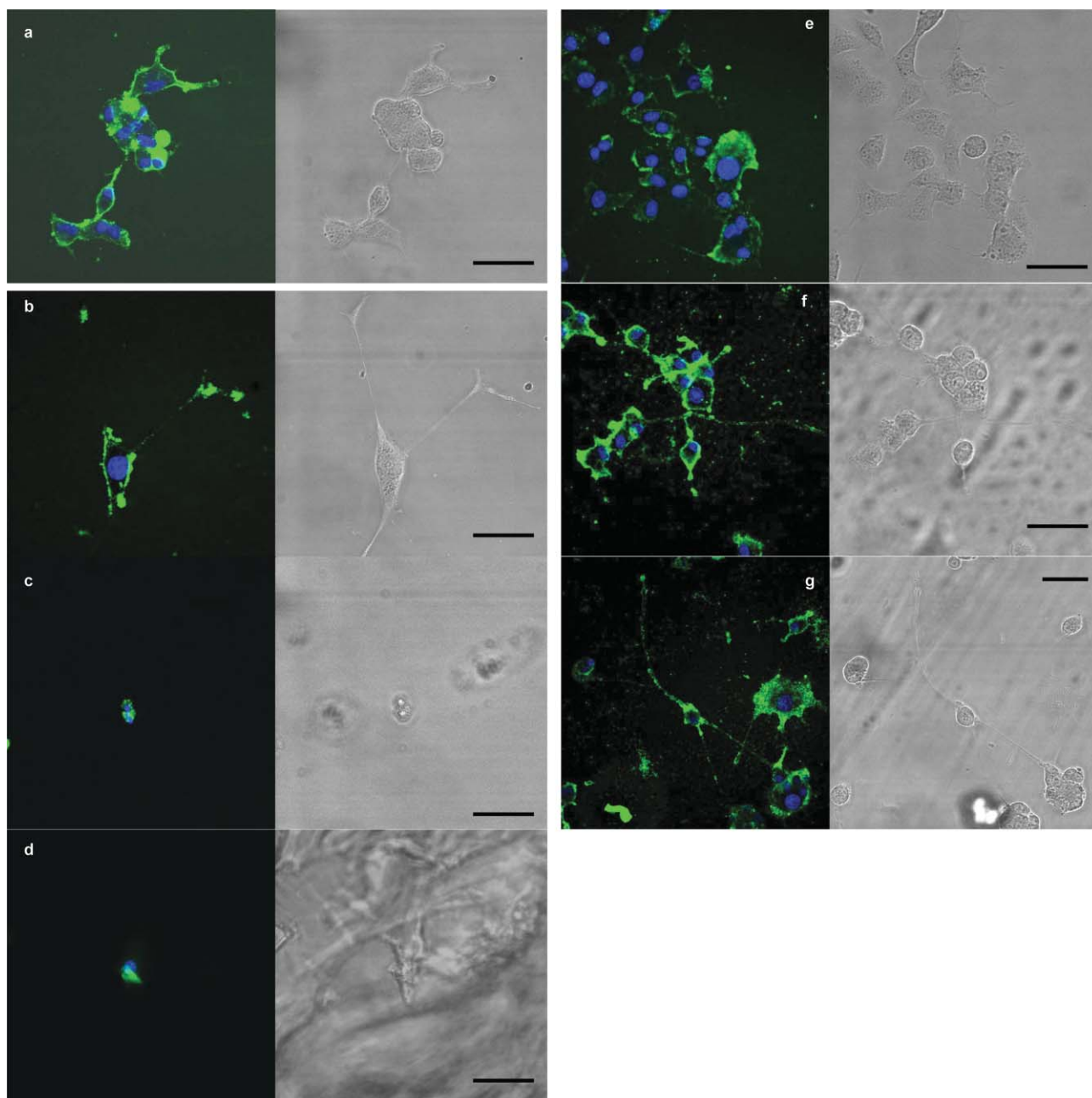
Fig. 4 Confocal images of PC12 cells on sol-gel surfaces. Cells were stained with FM1-43 and Hoechst 43382. (A) Cleaned glass control. (B) Cleaned glass control coated with 0.01% PLL. (C) TMOS bulk gel. (D) TMOS bulk gel doped with 0.01% poly-L-lysine. (E) TMOS thin film. (F, G) TMOS thin film doped with 0.01% poly-L-lysine. (Scale bar = 50 μm.)

study highlight the complexity of the neuronal phenotype and the importance of examining the signaling mechanisms linking material properties to cellular function.

The development of mature presynaptic neurotransmitter mechanisms as well as cell to cell synaptic connections are the ultimate goal of neuronal differentiation for many biomedical devices, implants, and biosensors. Neurotransmitter release or synaptic activity may be more relevant measures for assessing neuronal differentiation studies on biomaterials. Understanding the impact of sol-gel material properties on these functional neuronal ''markers'' will be the focus of future work.

Experimental

Preparation of materials

The precursor sol was prepared by combining 3.8 mL of tetramethoxysilane (TMOS) to 850 μL ddH$_2$O. 55 μL 0.04 N HCl was added to catalyze hydrolysis. The mixture was sonicated for 15 min, allowing for near-complete hydrolysis of the TMOS sol. The mixture was then filtered (0.2 μm Whatman syringe filter) in a sterile hood to ensure sterility for cell culture. Following filtration, several types of substrate were prepared. Native TMOS thin films and bulk materials were prepared as discussed below. In addition, bulk materials
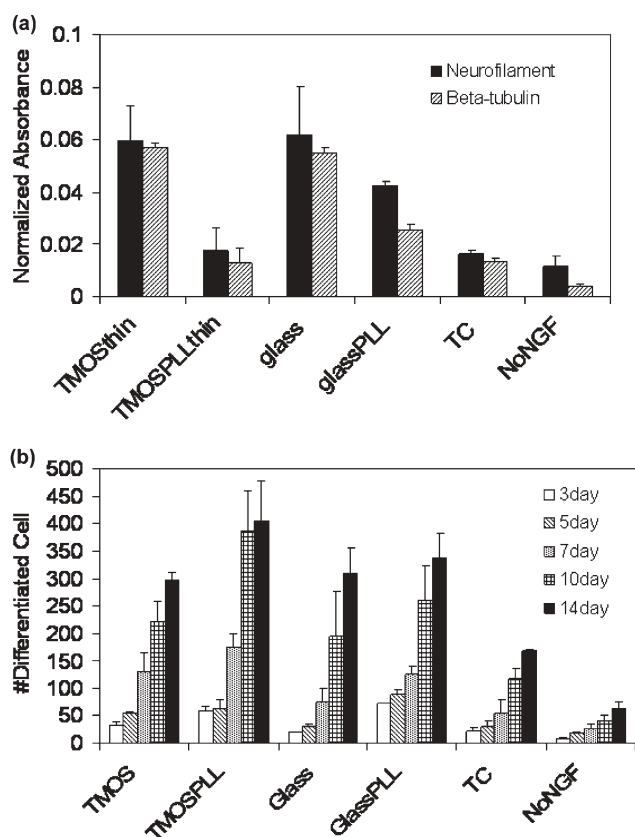
Fig. 5 Differentiation counts and ELISA data. (a) ELISA data were collected for beta-tubulin and neurofilament proteins, and the antibody reactions were quantified using o-phenylenediamine reaction with HRP. Absorbance values were collected at 490 nm and normalized to the number of cells determined by the CyQUANT assay. The TMOS thin films had the highest expression level of both of the differentiation markers. As expected, the cells that were not induced with NGF have very little expression of the markers. A student's t-test was performed between the TMOS $\pm$ PLL ($\alpha<0.05$) samples. Additionally, the glass samples were compared to the tissue culture (TC) and the glass + PLL samples ($\alpha<0.05$). The * represents a significant difference. (b) Differentiated cells were counted at several time points through the course of the experiment. Differentiated cells are defined as cells extending at least one neurite at least as long as the cell body. Cells were examined under a $20 \times$ objective, and at least three fields of view were averaged for each well. Three wells of each condition were examined for each experiment and all values averaged and multiplied by the total well area to achieve differentiation counts. The number of cells that appear to be differentiated do not correlate with the differentiation marker analysis.

and thin films were prepared with a final concentration of 0.01% poly-L-lysine (PLL). The PLL was added into the buffer prior to gel condensation.

For preparation of the thin film substrate support, VWR micro glass cover slips (0.13 mm thick) were cut to fit the desired plate size and cleaned in hot piranha solution (1 : 4 H_2O_2 : H_2SO_4 by volume) for 30 min. The cover slips were then rinsed several times in distilled water, followed by several rinses in ddH$_2$O with a final sonication in ddH$_2$O for 10 min. Cover slips were dried quickly under nitrogen and used immediately. Thin films were produced by dip coating using a lab developed dip-coating apparatus. The glass cover slips

were dipped at a controlled rate of 35 mm s^{-1} in a sterilized mixture of 30% TMOS sol, 70% 0.2 M phosphate buffer (pH 6.0, sterile-filtered), with an additional 10% of the final volume of methanol added to slow gelation. Films were briefly allowed to gel, and then placed in sterile buffer for use. Films were sanitized in ethanol for 15 min prior to preparation for cell seeding. Films were examined at $20 \times$ magnification for quality control purposes. Films that were cracked or flaking from the glass base were not used.

Bulk materials were cast by preparing a sterile mixture of 30% TMOS sol and 70% 0.2 M phosphate buffer (pH 6.0) and an additional 10% of the final volume of methanol directly in sterile culture dishes. For 12 well culture dishes (BD Falcon), 700 µL of the mixture was used, in 96-well plates (BD Falcon), 45 µL of the mixture was used. The mixture was allowed to gel and immediately covered with PBS, pH 7.4 (Mediatech). The modifications made to the sol-gel procedure to ensure sterility did not appear to have an effect on the integrity of the sol-gel bulk materials or thin films.

For protein conformation analysis and cell culture studies, both types of substrates were rinsed several times with PBS (pH 7.4) and allowed to equilibrate in PBS for 24–48 h at 4 °C. This time period allowed for leaching and removal of alcohols resulting from gelation and sterilization of the materials. The gels used for protein conformational studies were then stored up to one week in phosphate buffer and used as prepared. For the gels used in cell culture, Ham's F12K supplemented with 10% heat-inactivated horse serum and 5% fetal bovine serum was placed on the gels, and incubated at 37 °C for 6 h. The medium was removed and cells were seeded directly onto the substrates without rinsing. The extensive washing of the materials in PBS prior to media equilibration and cell seeding was critical for cell survival. The methanol produced during sol-gel synthesis and the ethanol used to sanitize the thin films is toxic to cells and can cause protein denaturation and precipitation, thus, the alcohols must be thoroughly removed from the materials. The time for washing exceeded that necessary for the thin films, however, the bulk materials require extensive time in PBS to remove the methanol from the sol-gel matrix, as the diffusion through the thick porous material is extremely slow. The equilibration with the culture media is also essential for successfully culturing the cells. The culture media provides a protein layer for the cells to seed upon as well as equilibrates the bulk material pores with the media components to prevent excess PBS from entering the cell culture environment and diluting the cell media.

Materials characterization–atomic force microscopy

Native TMOS thin films and bulk materials were imaged in buffer using a fluid cell and a closed-loop atomic force microscope (Asylum Research) operating in AC-mode. The AFM was used to determine the differences in nano-topographical characteristics of the gels. Bulk gels were cast in 1 mm protein gel cassettes under sterile conditions and carefully sliced into 50 mm squares. The thin films were prepared using filtered materials (0.2 µm pore size) as described and transferred to a sterile hood. After preparation, both types of gels were quickly attached to a glass window of

This journal is © The Royal Society of Chemistry 2006

J. Mater. Chem., 2006, **16**, 3221–3230 | 3227

the fluid cell with waterproof, fast setting resin-based adhesive. After allowing 15–30 s to adhere, the samples then were placed in gel purified pH 7.4 phosphate buffer. The gels were rinse and transferred to clean buffer, to prevent any resin byproducts from interfering with the gel structure. Samples was sealed into the fluid cell, immediately filled with the phosphate buffer, and imaged. For all imaging experiments, 60 μm long SiN bio-lever probes (Olympus) with a 0.027 N m^{-1} spring constant were used and Z-series, phase, and amplitude traces and retraces were collected and compared. The probe-tips had an approximate radius of curvature of 40 nm. The 512 × 512 pixel images were scanned at a rate of 1 Hz. The images were flattened under a first order correction and analyzed for height distributions using IgorPro software.

Fibronectin labeling

Human plasma fibronectin (Chemicon, Temecula, CA) was labeled using the method of Baneyx, Baugh & Vogel,[49] with a few modifications. Fibronectin at 2 mg ml^{-1} in phosphate buffer (pH 7.4) was first denatured at 4 M guanidine hydrochloride (Fluka) for 15 min. Following denaturation, the acceptor molecule, sulfhydryl reactive AlexaFluor 546 maleimide (Molecular Probes, Carlsbad, CA) was added at a ten-fold molar excess, mixed gently, and allowed to react for 1 h. The reaction resulted in two labeled cysteine residues per fibronectin subunit, located in modules FnIII$_7$ and FnIII$_{15}$.[48] The protein was then dialyzed (Pierce Slide-A-Lyzer) using dialysis cassettes, MW cutoff 10,000 Da against phosphate buffer with 0.1 M sodium bicarbonate (pH 8.5) for 4 h at room temperature, with three changes of buffer. This procedure refolds the fibronectin to a native state. Following the dialysis, the protein is further reacted with donor molecules (amine reactive AlexaFluor 488 carboxylic acid (Molecular Probes)) at a 40 fold molar excess. The reaction is mixed gently and allowed to react for 1 h. Excess label was purified by passing through a size-exclusion chromatography column using Sephadex G25 (Amersham Biosciences). The number of labels and protein concentration were determined at each step using a Cary 50 spectrophotometer (Varian Instruments) to determine absorbtion at λ_{280}, λ_{495}, and λ_{546}.

Characterization of labeled fibronectin

Labeled fibronectin was characterized using two methods. First, labeled fibronectin was characterized using an upright Nikon Labophot fluorescence microscope with a PARISS (Prism and Reflector Imaging Spectroscopy System) imaging spectrometer (LightForm, Inc.) attached. Doubly labeled fibronectin was denatured using 0–6 M guanidine hydro-chloride for 10 min, placed on a poly(ethylene glycol) (PEG) coated slide to prevent protein adsorption, and the spectra were collected using a mercury arc lamp and an excitation wavelength of 488 nm. A 488 nm short-pass, 45° dichroic filter was used to separate excitation and emission light. PEG coated slides were prepared using published methods.[69,70] A PEG coated surface has been shown to resist protein adsorption; allowing the protein to remain in native solution state so that accurate protein folding data can be collected. The spectra at various denaturant concentrations were collected.

Circular dichroic spectra (Jasco J810 CD Spectro-polarimeter) were collected from the labeled fibronectin and compared to native fibronectin in solution. Fibronectin, at 0.05 mg ml^{-1} in phosphate buffer was scanned in a quartz cell with a 1.00 cm path length from 290–215 nm at progressive denaturation conditions (0–6 M) using guanidine hydro-chloride. CD peaks (mdeg) were collected at 228 nm and compared across the denaturant conditions. Both native and labeled fibronectin were scanned through at least five denaturation series.

FRET on substrates

To assess protein structure on sol-gel surfaces, spectra from the labeled protein were obtained using PARISS. Protein was allowed to adsorb to the various bulk material and thin film surfaces at a concentration of 2 μg mL^{-1} in 0.2 M phosphate buffer (pH 7.4). This concentration was chosen to simulate a monolayer while still providing a good signal for collection. This also avoids molecular packing, which has been shown to prevent denaturation.[71–73] Spectra were collected from 400 nm to 600 nm, using the PARISS setup and Image-Pro Plus Software (Media Cybernetics, Inc.). The spectral system calibration was performed using the Multi-Ion Discharge Lamp (MIDL) (Lightform, inc). Each spectrum was collected over five sections of each gel, and at least four gels prepared on three separate dates were analyzed, for a total of 60 spectra collected on each material type.

PC12 cell culture

Rat pheochromocytoma (PC12) cells (ATCC #CRL-1721) were prepared for differentiation studies by culturing on 10 cm culture dishes coated with 0.05 mg ml^{-1} collagen (Becton Dickinson). Cells (1 × 10^6 cells/dish) were grown in an undifferentiated state until transfer to substrates for differen-tiation studies. Cells were maintained in Ham's F12K medium (ATCC), supplemented with 10% heat-inactivated horse serum (Invitrogen), 5% fetal bovine serum (Invitrogen), and 1% penicillin-streptomycin (Sigma). Cells were passaged approxi-mately every 96 h, or at 80% confluency using standard trypsin techniques.

Following preparation of substrates, PC12 cells were removed from the culture dishes using 0.05% trypsin/ 0.53 mM EDTA (Mediatech Herndon, VA). Cells were plated at a density of 25,000 cells cm^{-2} and maintained on substrates in Ham's F12K supplemented with 1% fetal bovine serum, 1% penicillin-streptomycin, and 50 ng ml^{-1} nerve growth factor (Invitrogen) to induce differentiation into a neuronal pheno-type. Media were replaced every two days and cells were allowed to differentiate for seven days prior to analysis.

Differentiation studies

Cells were assessed for differentiation using several methods. Cells were examined under light microscopy (Leica DM IRB) and representative cells were imaged using an attached Hamamatsu camera and ImagePro Software. Typically, neuronal phenotypes are assessed using neurite length or cell attachment counts; however, many of the substrates produce

tightly packed clusters of cells, making assessment inaccurate and difficult. The number of cells expressing differentiation characteristics (flattening or neurite extensions) was quantified by counting three representative fields of view with 20–30 cells at days 3, 5, 7, 10, and 14 in culture under $20\times$ magnifications. These fields of view were averaged and quantified for the entire area of the substrate to generate a differentiation count over time.

Due to the cell clumping, laser scanning confocal microscopy was also used to examine the cell numbers. Staining was accomplished by incubating live cells with FM1-43 dye and Hoechst 33342 (Molecular Probes) for five min immediately followed by imaging. Confocal images were acquired using a Bio-Rad Radiance Multiphoton confocal microscope with a $20\times$ Zeiss objective.

ELISA (Enzyme-linked immunosorbent assay) was used to assess protein signaling related to differentiation of PC12 cells induced by nerve growth factor. Neurofilament proteins and β-tubulin isotype III are increased during nerve growth factor differentiation of PC12 cells and were chosen to assess neuronal differentiation.[74] Cells were cultured on substrates in 96 well plates for 14 days under standard culture conditions. Control cells were cultured on tissue culture plastic and maintained under identical culture conditions, but without the NGF. Following culture, the cells were processed for ELISA.[74] The cells were fixed on the substrates in the original plates with 4% paraformaldehyde (Sigma Aldrich, St. Louis, MO), followed by 100% methanol (Sigma). The cells were then blocked with 10% FBS (Mediatech) in DPBS for 1 h. Biotinylated antibodies to neurofilament proteins (AFFINITI research) and β-tubulin isotype III (Sigma) were added at a 1 : 500 dilution in 10% FBS and incubated for 1 h. The antibodies were biotinylated using a NH_2 reactive biotin labeling kit with the standard protocol provided by Dojindo Molecular Technologies (Gaithersburg, MD). Following the primary antibody, the cells were reacted with avidin conjugated horseradish peroxidase (avidin-HRP) (Zymed, San Francisco, CA). The cells were rinsed and bound HRP activity was detected by reaction with 0.4 mg ml^{-1} o-phenylenediamine (OPD) (Sigma) containing 0.01% H_2O_2 in DPBS for 15 min. The reaction was subsequently stopped with the addition of 8 N H_2SO_4. The optical density of each of the wells was read at 490 nm using a microplate reader (Molecular Devices Spectramax). The OD values were normalized by the number of cells.

Cells were quantified on the various substrates using the CyQUANT cell proliferation assay provided by Molecular Probes (Eugene, OR). Cells were cultured on substrates in 96 well opaque plates (Costar) for 14 days under conditions described above. Following the culture period, the media was aspirated off the cells and the cells were rinsed once with PBS. The original plates containing the sol-gel materials were frozen at -70 °C for 24 h. The standard curve was generated using PC12 cells at the same passage number as the cells being studied, and the cells were counted using the standard protocol provided by Molecular Probes. The fluorescence intensity of each well was measured with a microplate fluorescence spectrometer (Molecular Devices FlexStation II) by exciting the dye at 485 nm and collecting the emission intensity at 530 nm. Each differentiation and cell counting experiment was averaged over three different culture wells prepared on four separate dates, for a total of 12 separate experiments.

Conclusions

The design of sol-gel materials as a biointerface for adherent mammalian cells will depend upon the particular cell type and desired function for the interface. A fundamental understanding of how the material properties impact the cellular state will be required for the rational design of such materials. This work demonstrates that future neuronal sol-gel interfaces need to consider the surface topography of sol-gel materials in addition to the surface chemistry. These considerations should direct choices regarding precursor chemistry, processing methods, and post-synthesis modifications.

References

1 C. Zolkov, D. Avnir and R. Armon, *J. Mater. Chem.*, 2004, **14**, 2200–2205.
2 S. Braun, S. Shtelzer, S. Rappoport, D. Avnir and M. Ottolenghi, *J. Non-Cryst. Solids*, 1992, **147&148**, 739–743.
3 L. M. Ellerby, C. R. Nishida, F. Nishida, S. A. Yamanaka, B. Dunn, J. S. Valentine and J. I. Zink, *Science*, 1992, **255**, 1113–1115.
4 B. J. Nablo and M. H. Schoenfisch, *Biomaterials*, 2005, **26**, 21, 4405–4415.
5 T. Besanger, Y. Zhang and J. D. Brennan, *J. Phys. Chem. B*, 2002, **106**, 10535–10542.
6 T.-J. M. Luo, R. Soong, E. lan, B. Dunn and C. Montemagno, *Nat. Mater.*, 2005, **4**, 220–224.
7 J. Zhao, S. Jedlicka, J. Lannu, A. K. Bhunia and J. L. Rickus, *Biotechnol. Prog.*, 2006, **22**, 32–37.
8 T. R. Besanger, B. Easwaramoorthy and J. D. Brennan, *Anal. Chem.*, 2004, **76**, 21, 6470–6475.
9 L. Inama, S. Dire, G. Carturan and A. Cavazza, *J. Biotechnol.*, 1993, **30**, 2, 197–210.
10 N. Nassif, O. Bouvet, M. N. Rager, C. Roux, T. Coradin and J. Livage, *Nat. Mater.*, 2002, 1.
11 V. M. Sglavo, G. Carturan, r. D. Monte and M. Muraca, *J. Mater. Sci.*, 1999, **34**, 3587–3590.
12 M. Muraca, M. T. Vilei, G. E. Zanusso, C. Ferraresso, S. Boninsegna, R. Dal Monte, P. Carraro and G. Carturan, *Artif. Organs*, 2002, **26**, 8, 664–669.
13 T. O. Shinji Sakai, Hiroyuki Ijima and Koei Kawakami, *J. Biomater. Sci., Polym. Ed.*, 2003, **14**, 7, 643–652.
14 X. Chen, J. Jia and S. Dong, *Electroanalysis*, 2003, **15**, 7, 608–612.
15 R. Igreja, C. J. Dias and J. N. Marat-Mendes, *Key Eng. Mater.*, 2002, **230–232**, 177–180.
16 J. R. Jones and L. L. Hench, *J. Mater. Sci.*, 2003, **38**, 18, 3783–3790.

This journal is © The Royal Society of Chemistry 2006

J. Mater. Chem., 2006, **16**, 3221–3230 | 3229

17 D. Avnir, V. R. Kaufman and R. Reisfeld, *J. Non-Cryst. Solids*, 1985, **74**, 395–406.

18 D. Avnir, T. Coradin, O. Lev and J. Livage, *J. Mater. Chem.*, 2006, **16**, 1013–1030.

19 P. Sepulveda, J. R. Jones and L. L. Hench, *J. Biomed. Mat. Res.*, 2002, **59**, 2, 340–348.

20 J. L. Rickus, P. J. Lee, P. L. Chang, A. J. Tobin, J. I. Zink and B. Dunn, unpublished data.

21 B. Dunn and J. I. Zink, *Chem. Mater.*, 1997, **9**, 11, 2280–2291.

22 M. H. Huang, H. M. Soyez, B. S. Dunn and J. I. Zink, *Chem. Mater.*, 2000, **12**, 1, 231–235.

23 D. S. Gottfried, A. Kagan, B. M. Hoffman and J. M. Friedman, *J. Phys. Chem.*, 1999, **103**, 2803–2807.

24 J. D. Brennan, K. K. Flora, G. N. Bendiak, G. A. Baker, M. A. Kane, S. Pandey and F. V. Bright, *J. Phys. Chem.*, 2000, **104**, 10100–10110.

25 J. Sui, D. Tleugabulova and J. D. Brennan, *Langmuir*, 2005, **21**, 4996–5001.

26 N. Faucheux, R. Schweiss, K. Lutzow, C. Werner and T. Groth, *Biomaterials*, 2004, **25**, 2721–2730.

27 Y. Bledi, A. J. Domb and M. Linial, *Brain Res. Proto.*, 2000, **5**, 282–289.

28 M. W. Hayman, K. H. Smith, N. R. Cameron and S. A. Przyborski, *J. Biochem. Biophys. Methods*, 2005, **62**, 231–240.

29 V. P. Shastri, *Curr. Pharm. Biotechnol.*, 2003, **4**, 331–337.

30 N. R. Washburn, K. M. Yamada, C. G. J. Simon, S. B. Kennedy and E. J. Amis, *Biomaterials*, 2004, **25**, 1215–1224.

31 A. Girotti, J. Reguera, F. J. Arias, M. Alonso and A. M. Testera, *J. Mater. Sci. 2003*, 2004, **15**, 4, 479–484.

32 P. A. Ramires, M. A. M., E. Panzarini, L. Dini and C. Protopapa, *J. Biomed. Mater. Res. B: Appl. Biomater.*, 2005, **72B**, 2, 230–238.

33 W. G. Brodbeck, M. S. Shive, E. Colton, Y. Nakayama, T. Matsuda and J. M. Anderson, *J. Biomed. Mater. Res.*, 2001, **55**, 661–668.

34 B. G. Keselowsky, D. M. Collard and A. J. Garcia, *J. Biomed. Mater. Res.*, 2003, **66A**, 247–259.

35 M. Shen and T. A. Horbett, *J. Biomed. Mater. Res.*, 2001, **57**, 336–345.

36 C. H. Thomas, C. D. McFarland, M. L. Jenkins, A. Rezania, J. G. Steele and K. E. Healy, *J. Biomed. Mater. Res.*, 1997, **37**, 81–93.

37 B. Baharlo, M. Textor and D. M. Brunette, *J. Biomed. Mater. Res.*, 2005, **74A**, 12–22.

38 A. J. Garcia, M. D. Vega and D. Boettiger, *Mol. Biol. Cell*, 1999, **10**, 785–798.

39 J. Sottile and D. C. Hocking, *Mol. Biol. Cell*, 2002, **13**, 3546–3559.

40 S. M. Cutler and A. J. Garcia, *Biomaterials*, 2003, **24**, 1759–1770.

41 D. E. MacDonald, N. Deo, B. Markovic, M. Stranick and P. Somasundaran, *Biomaterials*, 2002, **23**, 1269–1279.

42 M. Conti, G. Donati, G. Cianciolo, S. Stefoni and B. Samori, *J. Biomed. Mater. Res.*, 2002, **61**, 370–379.

43 L. Baugh and V. Vogel, *J. Biomed. Mater. Res.*, 2004, **69A**, 3, 525–534.

44 A. K. Harris, *J. Biotechnol. Eng.*, 1984, **106**, 19–24.

45 H. Liao, R. Bucala and R. A. Mitchell, *J. Biol. Chem.*, 2003, **278**, 1, 76–81.

46 B. Sim, J. Cladera and P. O'Shea, *J. Biomed. Mater. Res.*, 2004, **68A**, 2, 352–359.

47 R. T. T. Gettens, Z. Bai and J. L. Gilbert, *J. Biomed. Mater. Res.*, 2005, **72A**, 246–257.

48 G. Baneyx, L. Baugh and V. Vogel, *Proc. Natl. Acad. Sci. U. S. A.*, 2001, **98**, 25, 14464–14468.

49 G. Baneyx, L. Baugh and V. Vogel, *Proc. Natl. Acad. Sci. U. S. A.*, 2002, **99**, 8, 5139–5143.

50 E. Cota and J. Clarke, *Protein Sci.*, 2000, **9**, 112–120.

51 L. A. Greene, S. E. Farinelli, M. E. Cunningham and D. S. Park, Culture and the Experimental Use of the PC12 Rat Pheochromocytoma Cell Line in *Culturing Nerve Cells*, ed. G. Banker and K. Goslin, The MIT Press, Cambridge, 1998, pp 160–186.

52 A. A. J. Oliva, C. D. James, C. E. Kingman, H. G. Graighead and G. A. Banker, *Neurochem. Res.*, 2003, **28**, 11, 1639–1648.

53 H. K. Song, B. Toste, K. Ahmann, D. Hoffman-Kim and G. T. T. Palmore, *Biomaterials*, 2006, **27**, 473–484.

54 G. E. Park, M. A. Pattison, K. Park and T. J. Webster, *Biomaterials*, 2005, **26**, 16, 3075–3082.

55 D. C. Miller, K. M. Haberstroh and T. J. Webster, *J. Biomed. Mater. Res. Part A*, 2005, **73A**, 4, 476–484.

56 N. Pernodet, M. Rafailovich, J. Sokolov, D. Xu, N.-L. Yang and K. McLeod, *J. Biomed. Mat. Res.*, 2003, **64A**, 684–692.

57 L. Wicikowski, B. Kusz, L. Murawski, K. Szaniawska and B. Susha, *Vacuum*, 1999, **54**, 221–225.

58 G. Wu, J. Wang, J. Shen, T. Yang, Q. Zhang, B. Zhou, Z. Deng, B. Fan, D. Zhou and F. Zhang, *Mater. Res. Bull.*, 2001, **36**, 2127–2139.

59 S. V. Patwardhan and S. J. Clarson, *J. Inorg. Organomet. Polym.*, 2003, **11**, 3, 193–198.

60 N. Kroger, R. Deutzmann, C. Bergsdorf and M. Sumper, *Proc. Natl. Acad. Sci. U. S. A.*, 2000, **97**, 26, 14133–14138.

61 D. Lairez, E. Pauthe and J. Pelta, *Biophys. J.*, 2003, **84**, 6, 3904–3916.

62 E. T. W. Bampton and J. S. H. Taylor, *J. Neurobiol.*, 2005, **63**, 1, 29–48.

63 T. Kreis and R. Vale, *Guidebook to the Extracellular Matrix, Anchor, and Adhesion Proteins*, 2nd ed., Oxford University Press, New York, NY, 1999.

64 E. H. J. Danen and K. M. Yamada, *J. Cell Physiol.*, 2001, **189**, 1–13.

65 M. P. F., S. R., P. J., F. A. and O. M. M., *J. Neurosci. Res.*, 1993, **34**, 1, 129–134.

66 J. T. Yabe, W. K. H. Chan, T. M. Chylinski, S. Lee, A. F. Pimenta and T. B. Shea, *Cell Motil. Cytoskeleton*, 2001, **48**, 1, 61–83.

67 C. W. Jung, S. Lee, D. Ortiz, Q. Z. Zhu, J. P. Julien and T. B. Shea, *Mol. Brain Res.*, 2005, **141**, 2, 151–155.

68 P. R. Gordon-Weeks and I. Fischer, *Microsc. Res. Tech.*, 2000, **48**, 2, 63–74.

69 M. Zhang, T. Desai and M. Ferrari, *Biomaterials*, 1998, **19**, 953–960.

70 T. A. Desai, K. C. Popat and S. Sharma, *Business Briefing: Medical Device Manufacturing & Technology*, 2002, 1–4.

71 E. C. Williams, P. A. Janmey, J. D. Ferry and D. F. Mosher, *J. Biol. Chem.*, 1982, **257**, 24, 14973–14978.

72 L. Guemouri, J. Ogier, Z. Zekhnini and J. J. Ramsden, *J. Chem. Phys.*, 2000, **113**, 18, 8183–8186.

73 E. C. Williams, P. A. Janmey, J. D. Ferry and D. F. Mosher, *J. Biol. Chem.*, 1982, **257**, 24, 14973–14978.

74 T. Ohuchi, S. Maruoka, A. Sakuda and T. Arai, *J. Neurosci. Meth.*, 2002, **118**, 1–8.